

## 2-((1*H*-Azol-1-yl)methyl)-*N*-arylbenzamides: Novel dual inhibitors of VEGFR-1/2 kinases

Alexander S. Kiselyov,<sup>a,\*</sup> Marina Semenova,<sup>b</sup> Victor V. Semenov<sup>c</sup> and Evgueni Piatnitski<sup>d</sup>

<sup>a</sup>Small Molecule Drug Discovery, Chemical Diversity, Inc., 11558 Sorrento Valley Road, San Diego, CA 92121, USA

<sup>b</sup>Institute of Developmental Biology, Russian Academy of Sciences, 26 Vavilov Str., 119334 Moscow, Russia

<sup>c</sup>Zelinsky Institute of Organic Chemistry, Russian Academy of Sciences, 47 Leninsky Prospect, 117913 Moscow, Russia

<sup>d</sup>Small Molecule Drug Discovery, ImClone Systems, 180 Varick Street, New York, NY 10014, USA

Received 10 November 2005; revised 29 November 2005; accepted 30 November 2005

Available online 20 December 2005

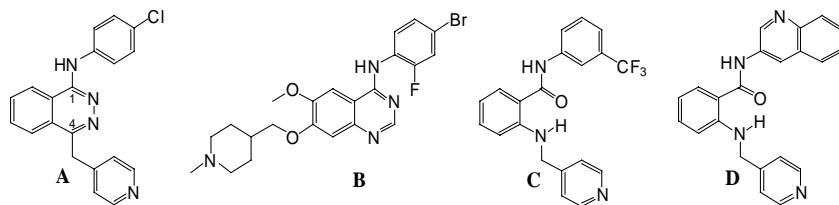
**Abstract**—Novel potent derivatives of (azol-1-yl)methyl-*N*-arylbenzamides with improved solubility (>3 mM) are described as ATP-competitive inhibitors of vascular endothelial growth factor receptor 2 (VEGFR-2). Many compounds display VEGFR-2 inhibitory activity reaching IC<sub>50</sub> < 100 nM in the enzymatic assay. The compounds also inhibit the related tyrosine kinase, VEGFR-1, with similar potencies. Several compounds containing bulky lipophilic substituents at the benzamide pharmacophore yielded 10- to 17-fold selectivity for the VEGFR-2 versus VEGFR-1 kinase.  
© 2005 Elsevier Ltd. All rights reserved.

Vascular endothelial growth factors (VEGFs) and their respective family of receptor tyrosine kinases (VEGFRs) are key proteins modulating angiogenesis, the formation of new vasculature from an existing vascular network.<sup>1</sup> Potent, specific, and non-toxic inhibitors of angiogenesis are powerful clinical tools in oncology and ophthalmology.<sup>2,3</sup> Several groups in industry have developed methods for sequestering VEGF. This leads to a signal blockade via VEGF receptors including both VEGFR-1 (Flt1) and VEGFR-2 (flk1, kinase insert domain receptor, KDR) and, subsequently to an inhibition of malignant angiogenesis.

There are reports describing small-molecule inhibitors that affect VEGF/VEGFR signaling by directly competing with the ATP-binding site of the respective intracellular kinase domain. This event leads to the inhibition of

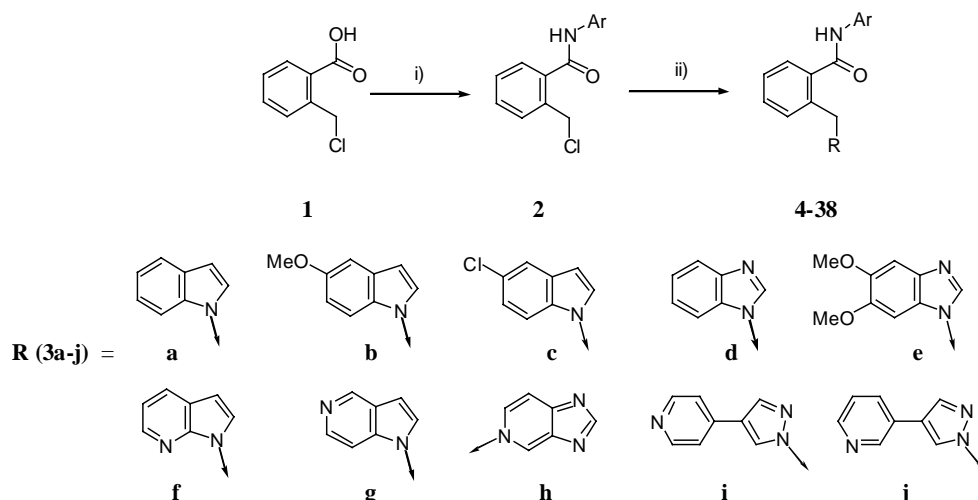
VEGFR phosphorylation and, ultimately to apoptotic death of the aberrant endothelial cells. Drug candidates that exhibit this mechanism of action include PTK 787 (Vatalanib™ **A**) and ZD 6474 (Vandetanib™ **B**). These are Phase III and II clinical candidates, respectively, against various cancers.<sup>4,5</sup> The six-membered ring of a phthalazine template in PTK 787 has been successfully replaced with the isosteric anthranil amide derivatives **C** and **D**. Intramolecular hydrogen bonding was suggested to be responsible for the optimal spatial orientation of pharmacophores, similar to the parent PTK 787.<sup>6</sup>

It has been suggested that the essential pharmacophores for the VEGFR-2 activity of phthalazines and their analogues include: (i) [6,6]fused (or related) aromatic system; (ii) *para*- or 3,4-di-substituted aniline function in



**Keywords:** Vascular endothelial growth factor receptor 2; Receptor tyrosine kinase; Dual kinase inhibitor; Angiogenesis; 2-((1*H*-Azol-1-yl)methyl)-*N*-arylbenzyl amides.

\* Corresponding author. Tel.: +1 858 794 4860; fax: +1 858 794 4931; e-mail: [ask@chemdiv.com](mailto:ask@chemdiv.com)



**Scheme 1.** Reagents and conditions: (i) DIC, ArNH<sub>2</sub>, CH<sub>2</sub>Cl<sub>2</sub>, rt, 2 h; (ii) **3a–j**, K<sub>2</sub>CO<sub>3</sub>, DMF, rt, 12 h.

**Table 1.** Activity of *N*-arylbenzamides **4–38** against VEGFR-2 and VEGFR-1 kinases

Compound	Ar	R	Observed (lit.) <sup>6</sup>	
			VEGFR-2, IC <sub>50</sub> <sup>a,b</sup> (μM)	VEGFR-1, IC <sub>50</sub> <sup>a,b</sup> (μM)
A, PTK787			0.054 ± 0.006 (0.042 ± 0.003)	0.14 ± 0.02 (0.11 ± 0.03)
B, ZD6474			0.022 ± 0.003 (0.017 ± 0.003)	0.10 ± 0.01 (0.09 ± 0.01)
C			0.032 ± 0.005 (0.023 ± 0.006)	0.17 ± 0.05 (0.130 ± 0.081)
D			0.015 ± 0.004 (0.009 ± 0.001)	0.16 ± 0.05 (0.13 ± 0.03)
4	4-Cl(C <sub>6</sub> H <sub>4</sub> )	a	>10	>10
5	4-Cl(C <sub>6</sub> H <sub>4</sub> )	b	>10	>10
6	4-Cl(C <sub>6</sub> H <sub>4</sub> )	c	>10	>10
7	4-Cl(C <sub>6</sub> H <sub>4</sub> )	d	>10	>10
8	4-Cl(C <sub>6</sub> H <sub>4</sub> )	e	3.55 ± 0.50	>10
9	4-Cl(C <sub>6</sub> H <sub>4</sub> )	f	>10	>10
10	4-Cl(C <sub>6</sub> H <sub>4</sub> )	g	0.092 ± 0.008	0.22 ± 0.07
11	4-Cl(C <sub>6</sub> H <sub>4</sub> )	h	0.047 ± 0.005	0.14 ± 0.02
12	4-Cl(C <sub>6</sub> H <sub>4</sub> )	i	4.28 ± 0.66	>10
13	4-Cl(C <sub>6</sub> H <sub>4</sub> )	j	>10	>10
14	4- <i>t</i> -Bu(C <sub>6</sub> H <sub>4</sub> )	g	0.052 ± 0.006	0.76 ± 0.08
15	4- <i>t</i> -Bu(C <sub>6</sub> H <sub>4</sub> )	h	0.061 ± 0.006	0.61 ± 0.07
16	4- <i>i</i> -Pr(C <sub>6</sub> H <sub>4</sub> )	g	0.087 ± 0.008	0.54 ± 0.07
17	4- <i>i</i> -Pr(C <sub>6</sub> H <sub>4</sub> )	h	0.11 ± 0.01	0.44 ± 0.06
18	4-ClF <sub>2</sub> CO(C <sub>6</sub> H <sub>4</sub> )	g	<b>0.073 ± 0.02</b>	<b>1.25 ± 0.12</b>
19	4-ClF <sub>2</sub> CO(C <sub>6</sub> H <sub>4</sub> )	h	<b>0.095 ± 0.02</b>	<b>1.16 ± 0.11</b>
20	3-Me(C <sub>6</sub> H <sub>4</sub> )	g	0.47 ± 0.07	0.74 ± 0.10
21	3-Me(C <sub>6</sub> H <sub>4</sub> )	h	0.35 ± 0.06	0.57 ± 0.08
22	2-Me(C <sub>6</sub> H <sub>4</sub> )	g	>10	>10
23	2-Me(C <sub>6</sub> H <sub>4</sub> )	h	>10	>10
24	4- <i>N</i> -Morpholino-(C <sub>6</sub> H <sub>4</sub> )	g	0.28 ± 0.04	0.34 ± 0.04
25	4- <i>N</i> -Morpholino-(C <sub>6</sub> H <sub>4</sub> )	h	0.21 ± 0.04	0.30 ± 0.05
26	3,4-Cl(C <sub>6</sub> H <sub>4</sub> )	g	0.066 ± 0.008	0.22 ± 0.04
27	3,4-Cl(C <sub>6</sub> H <sub>4</sub> )	h	0.056 ± 0.008	0.26 ± 0.05
28	4-Cl-3-CF <sub>3</sub> (C <sub>6</sub> H <sub>3</sub> )	g	0.31 ± 0.03	0.41 ± 0.07
29	4-Cl-3-CF <sub>3</sub> (C <sub>6</sub> H <sub>3</sub> )	h	0.44 ± 0.05	0.69 ± 0.09
30	2-F-4-Me(C <sub>6</sub> H <sub>3</sub> )	g	0.29 ± 0.03	0.34 ± 0.05
31	2-F-4-Me(C <sub>6</sub> H <sub>3</sub> )	h	0.21 ± 0.04	0.49 ± 0.06
32	3,4-Methylenedioxy	g	0.13 ± 0.02	0.18 ± 0.03
33	3,4-Methylenedioxy	h	0.23 ± 0.04	0.36 ± 0.05
34	4-Br(C <sub>6</sub> H <sub>4</sub> )	g	0.44 ± 0.08	0.95 ± 0.11
35	4-Br(C <sub>6</sub> H <sub>4</sub> )	h	0.38 ± 0.06	0.77 ± 0.09
36	4-Ph(C <sub>6</sub> H <sub>4</sub> )	h	0.69 ± 0.09	1.14 ± 0.15
37	4-PhO(C <sub>6</sub> H <sub>4</sub> )	h	1.55 ± 0.22	2.53 ± 0.31
38	4-Bn(C <sub>6</sub> H <sub>4</sub> )	h	2.12 ± 0.35	>10

<sup>a</sup> IC<sub>50</sub> values were determined from the logarithmic concentration–inhibition curves (10 points). The values are given as means of at least two duplicate experiments.

<sup>b</sup> Lit. IC<sub>50</sub> values, as measured at 8 μM ATP.<sup>6</sup>

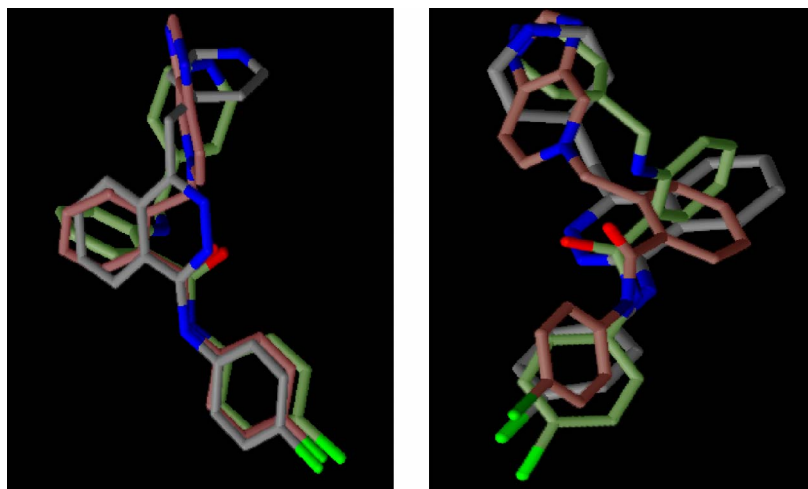


**Figure 1.** Structural overlap between inhibitor **11** (brown), PTK787 (**A**, gray), and **C** (green).

the position 1 of phthalazine; and (iii) hydrogen bond acceptor attached to the position 4 via an appropriate linker (aryl or fused aryl group).<sup>4,6</sup> To further assess structural requirements for the dual VEGFR1/VEGFR2 activity, we designed a set of molecules that have neither fused phthalazine system (**A**) nor the intramolecular hydrogen bonding (**C**, **D**).

The targeted 2-((1*H*-azol-1-yl)methyl)-*N*-arylbenzamide **4–38** (Scheme 1) were accessed by a three-step procedure. In the optimized procedure, *o*-chloromethyl benzoic acid (**1**) was reacted with a series of anilines in the presence of 1.2 equiv DIC in CH<sub>2</sub>Cl<sub>2</sub> to give the respective amides (**2**) in 76–91% yields. Alternative amine coupling procedures involving DMAP, carbonyl diimidazole, and benzotriazole afforded lower yields of **2**. The resultant chlorides were reacted with anions generated in situ from the respective NH heterocycle (**3a–j**) in DMF to furnish the targeted molecules **4–38** (45–64% isolated yields). Notably, reactions of **2** with 3*H*-imidazo[4,5-*c*]pyridine in the presence of K<sub>2</sub>CO<sub>3</sub> furnished products of a formal S<sub>N</sub>2 of chloride **2** with pyridine-, instead of the anticipated imidazole-nitrogen atom attack (e.g., **11**, Table 1). The latter derivatives were not detected in the reaction mixtures by LC–MS. Structures of the resultant products were further confirmed by NOE experiments.<sup>7</sup>

Thirty-five compounds (**4–38**, Table 1) were tested in vitro against isolated VEGFR-2. Specifically, we measured their ability to inhibit phosphorylation of a biotinylated-polypeptide substrate (p-GAT, CIS Bio International) in a homogeneous time-resolved fluorescence (HTRF) assay at an ATP concentration of 2 μM. The results were reported as a 50% inhibition concentration value (IC<sub>50</sub>). Literature VEGFR-2 inhibitors (**A–D**) were included as internal standards for quality control.<sup>8</sup>

As seen from Table 1, a number of 2-((1*H*-azol-1-yl)methyl)-*N*-arylbenzamide exhibited robust inhibitory activity against VEGFR-2. By varying both amide- and (azol-1-yl)methyl substituents, it was

possible to modify compound potency against the enzyme. Initially, we selected benzamide pharmacophore (4-Cl-C<sub>6</sub>H<sub>4</sub>)<sup>6</sup> and studied the inhibitory effect of a heterocyclic substituent (**3a–3j**) on the enzymatic activity of the resultant compounds **4–13** against VEGFR-2. Two functions (**g**, **h**, Table 1) yielded compounds similar in potency to PTK787 (**10**, **11**; IC<sub>50</sub> = 92 and 47 nM, respectively). Weak activity was seen for the molecules **8** and **12** derived from **e** and **i**. Following these initial data, we decided to continue optimization of the molecules based on **g** and **h**. Good potency of these series was explained by the proper alignment of the lower portion of the molecule, namely pyridine-type nitrogen atom(s) of a heterocycle (Lewis base: hydrogen bond acceptor), with the Arg1302 moiety in the ATP-binding pocket of VEGFR-2. This interaction may be critical for a tight binding of a phthalazine analogue to a VEGFR-2 kinase.<sup>9,10</sup> Furthermore, MMFF94 Force Field minimization studies suggest good overlap between series described in this paper, as exemplified by **11** and the development candidates PTK787 (**A**) and (**C**) (Fig. 1).

In the next step, we focused on studying SAR of the amide portion of the molecule. The molecules substituted with *p*-Cl-, *p*-*t*-Bu-, and *p*-*i*-Pr- groups displayed potencies similar to those of **C** and PTK787 with IC<sub>50</sub> values of 47–92 nM in the enzymatic assay (e.g., **10**, **11**, and **14–17**, Table 1).<sup>6</sup> The (difluorochloro)methoxy group (ClF<sub>2</sub>CO-, compounds **18**, **19**, IC<sub>50</sub> = 73 and 95 nM, respectively) was also beneficial for VEGFR-2 inhibition. Small *meta*-substituents on the anilinic portion of the molecule were tolerated (**20**, **21**, IC<sub>50</sub> = 0.47 and 0.35 μM, respectively). Similar *ortho*-substitution abolished enzymatic inhibition (**22**, **23**; IC<sub>50</sub> > 10 μM for both). Several di-substituted aniline fragments, for example, 3,4-di-Cl- (**26**, **27**; IC<sub>50</sub> = 66 and 56 nM, respectively), 4-Cl-3-CF<sub>3</sub>- (**28**, **29**, IC<sub>50</sub> = 0.31 and 0.44 μM, respectively), 2-F-4-Me- (**30**, **31**; IC<sub>50</sub> = 0.29 and 0.21 μM, respectively), and 3,4-methylenedioxy groups (**32**, **33**; IC<sub>50</sub> = 0.13 and 0.23 μM, respectively) also yielded potent compounds. Related *ortho*-fluoro aminoaryl group has been exemplified in other VEGFR-2 inhibitors such as ZD 6474.<sup>5</sup> Larger 4-substituents

**Table 2.** Compounds **11**, **14**, **18**, **19**, and **26** are ATP-competitive inhibitors of VEGFR-2

Compound	$K_i$ at $IC_{50}$ ( $\mu$ M)	$K_i$ at $IC_{90}$ ( $\mu$ M)
<b>11</b>	0.09	0.11
<b>14</b>	0.13	0.15
<b>18</b>	0.16	0.21
<b>19</b>	0.22	0.19
<b>26</b>	0.17	0.21

on the arylamide portion of the molecule led to a diminished potency against the enzyme (**34–38**). For example, 4-Br derivatives (**34**, **35**) lost almost 5-fold of activity compared to the 4-Cl analogues **10**, **11**. Phenyl, phenoxy, and benzyl derivatives (**36–38**) furnished only moderate potency against VEGFR-2. We speculated that these functions cannot be properly accommodated in the tight hydrophobic pocket of VEGFR-2.<sup>9</sup> Similar observation has been reported by the other group.<sup>4</sup> Three selected VEGFR-2 inhibitors, namely **11**, **14**, **18**, **19**, and **26**, all tested ATP-competitive in the radioassay<sup>11</sup> (see Table 2).

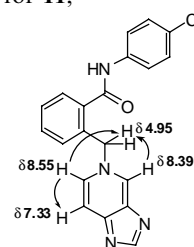
All compounds were also tested in the HTRF format against VEGFR-1. The results in Table 1 indicate that VEGFR-2 active *N*-arylbenzamides display good activity against VEGFR-1 as well. For the most active compounds, the  $IC_{50}$  values were in the 0.14–0.70  $\mu$ M range. This outcome could be of benefit in the clinical setting as both receptors are reported to mediate VEGF signaling in the angiogenesis.<sup>12</sup> Notably, several compounds containing bulky lipophilic substituents at the benzamide pharmacophore (**14–16**, **18**, and **19**) yielded 10- to 17-fold selectivity for the VEGFR-2 versus VEGFR-1 kinase. This observation suggests that it is possible to develop VEGFR-2 specific inhibitors decoupled from the VEGFR-1 activity. Further screening of **4–38** against a number of other receptor (IGF1R, InR, FGFR1, Flt3, ErbB1, ErbB2, EphB4, and c-Met) and cytosolic (PKA, GSK3 $\beta$ , PKB/Akt, bcr-Abl, and Cdk2/5) kinases in an HTRF format indicated no significant cross-reactivity (PI < 40%, triplicate measurements) at a screening concentration of 10  $\mu$ M.

In summary, we have described a series of 2-((1*H*-azolo-1-yl)methyl)-*N*-arylbenzamides as potent ATP-competitive inhibitors of the VEGFR-2 receptor. These compounds are also inhibitors of the VEGFR-1 receptor. All potent compounds are stable towards hydrolysis and display good solubility (>3 mM) in the screening buffer. The analogues presented in this Letter are potentially useful in the treatment of conditions such as cancer. Further details on their biological properties, such as cell-based and functional activity, together with murine oral exposure data, will be presented in due course.

## References and notes

- (a) Klagsbrun, M.; Moses, M. A. *Chem. Biol.* **1999**, *6*, R217; (b) Risau, W. *Nature* **1997**, *386*, 671.
- The anti-angiogenic antibody Avastin™ (Bevacizumab) has recently been approved to treat colorectal cancer; see: Culy, C. *Drugs Today* **2005**, *41*, 23.

- The anti-angiogenic aptamer Macugen™ (Pegaptanib sodium) has recently been approved to treat neovascular age-related macular degeneration; see: Fine, S. L.; Martin, D. F.; Kirkpatrick, P. *Nat. Rev. Drug. Discov.* **2005**, *4*, 187.
- Bold, G.; Altmann, K.-H.; Jorg, F.; Lang, M.; Manley, P. W.; Traxler, P.; Wietfeld, B.; Bruggen, J.; Buchdunger, E.; Cozens, R.; Ferrari, S.; Pascal, F.; Hofmann, F.; Martiny-Baron, G.; Mestan, J.; Rosel, J.; Sills, M.; Stover, D.; Acemoglu, F.; Boss, E.; Emmenegger, R.; Lasser, L.; Masso, E.; Roth, R.; Schlachter, C.; Vetterli, W.; Wyss, D.; Wood, J. M. *J. Med. Chem.* **2000**, *43*, 2310.
- (a) Hennequin, L. F.; Stokes, E. S. E.; Thomas, A. P.; Johnstone, C.; Ple, P. A.; Ogilvie, D. J.; Dukes, M.; Wedge, S. R.; Kendrew, J.; Curwen, J. O. *J. Med. Chem.* **2002**, *45*, 1300; (b) Wedge, S. R.; Kendrew, J.; Hennequin, L. F.; Valentine, P. J.; Barry, S. T.; Brave, S. R.; Smith, N. R.; James, N. H.; Dukes, M.; Curwen, J. O.; Chester, R.; Jackson, J. A.; Boffey, S. J.; Kilburn, L. L.; Barnett, S.; Richmond, G. H. P.; Wadsworth, P. F.; Walker, M.; Bigley, A. L.; Taylor, S. T.; Cooper, L.; Beck, S.; Juergensmeier, J. M.; Ogilvie, D. J. *Cancer Res.* **2005**, *65*, 4389.
- (a) Manley, P. W.; Furet, P.; Bold, G.; Brügggen, J.; Mestan, J.; Meyer, T.; Schnell, C.; Wood, J. *J. Med. Chem.* **2002**, *45*, 5697; (b) Manley, P. W.; Bold, G.; Fendrich, G.; Furet, P.; Mestan, J.; Meyer, T.; Meyhack, B.; Strauss, A.; Wood, J. *Cell Mol. Biol. Lett.* **2003**, *8*, 532; (c) Altmann, K.-H.; Bold, G.; Furet, P.; Manley, P. W.; Wood, J. M.; Ferrari, S.; Hofmann, F.; Mestan, J.; Huth, A.; Krüger, M.; Seidelmann, D.; Menrad, A.; Haberey, M.; Thierauch, K.-H. US Patent 6,878,720 B2, 2005.
- Similar reactivity of 3*H*-imidazo[4,5-*c*]pyridine toward electrophiles has been reported, see: (a) Ra, W. W. K.; Pacherb, K. G. R. *Tetrahedron* **1992**, *48*, 10549; (b) Penning, T. D.; Chandrakumar, N. S.; Desai, B. N.; Djuric, S. W.; Gasielki, A. F.; Malecha, J. W.; Miyashiro, J. M.; Russell, M. A.; Askonas, L. J.; Gierse, J. K.; Harding, E. I.; Highkin, M. K.; Kachur, J. F.; Kim, S. H.; Villani-Price, D.; Pyla, E. Y.; Ghoreishi-Haack, N. S.; Smith, W. G. *Bioorg. Med. Chem. Lett.* **2003**, *13*, 1137, Significant NOE's for **11**;



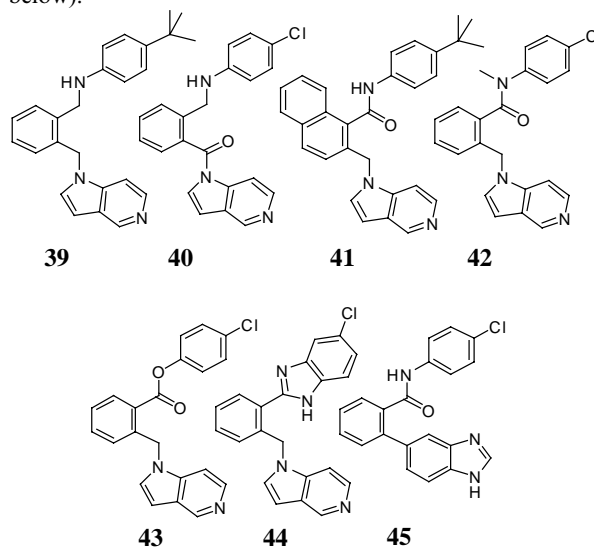
Tests revealed that all potent compounds were stable toward hydrolysis with amines (morpholine, piperazine), alkoxy- and hydroxide anions at reflux in MeOH/H<sub>2</sub>O and upon prolonged storage in DMSO. Furthermore, they displayed good solubility in the screening buffer (>3 mM) as indicated by HPLC studies.

**Analytical data for the selected compounds 8:** *N*-(4-Chlorophenyl)-2-((5,6-dimethoxy-1*H*-benzo[*d*]imidazol-1-yl)methyl)benzamide; mp 165–166 °C; <sup>1</sup>H NMR (400 MHz, DMSO-*d*<sub>6</sub>)  $\delta$ , ppm: 3.76 (s, 6H, OMe), 4.88 (s, 2H, CH<sub>2</sub>), 7.11 (s, 2H), 7.20 (d, *J* = 8.4 Hz, 1H), 7.23 (m, 1H), 7.26 (d, *J* = 8.4 Hz, 2H), 7.40 (m, 1H), 7.61 (d, *J* = 8.4 Hz, 2H), 7.75 (d, *J* = 8.4 Hz, 1H), 8.01 (s, 1H), 13.20 (br s, exch D<sub>2</sub>O, 1H, NH); <sup>13</sup>C NMR (100 MHz, DMSO-*d*<sub>6</sub>)  $\delta$ , ppm: 47.5, 56.6, 100.9, 122.6, 126.0, 127.3, 127.5, 128.7, 129.1, 129.4, 131.7, 132.1, 133.3, 133.9, 135.2, 141.4, 143.5, 165.0; ESI MS (*M*+1): 423, (*M*-1): 421; HRMS, exact mass calcd for C<sub>23</sub>H<sub>20</sub>ClN<sub>3</sub>O<sub>3</sub>: 421.1193. Found: 421.1185.

Elemental analysis Calcd for  $C_{23}H_{20}ClN_3O_3$ : C, 65.48; H, 4.78; N, 9.96. Found: C, 65.25; H, 4.97; N, 9.79. **10**: 2-((1*H*-Pyrrolo[3,2-*c*]pyridin-1-yl)methyl)-*N*-(4-chlorophenyl)benzamide; mp 174–175 °C;  $^1H$  NMR (400 MHz, DMSO-*d*<sub>6</sub>)  $\delta$ , ppm: 5.04 (s, 2H, CH<sub>2</sub>), 6.22 (d, *J* = 6.8 Hz, 1H), 6.68 (d, *J* = 6.8 Hz, 1H), 7.15 (d, *J* = 8.0 Hz, 1H), 7.19 (d, *J* = 8.4 Hz, 2H), 7.28 (m, 1H), 7.33 (d, *J* = 8.8 Hz, 1H), 7.41 (m, 1H), 7.60 (d, *J* = 8.4 Hz, 2H), 7.82 (d, *J* = 8.0 Hz, 1H), 8.33 (d, *J* = 8.8 Hz, 1H), 8.49 (s, 1H), 13.30 (br s, exch. D<sub>2</sub>O, 1H, NH);  $^{13}C$  NMR (100 MHz, DMSO-*d*<sub>6</sub>)  $\delta$ , ppm: 51.5, 98.9, 112.4, 121.6, 122.5, 124.9, 125.2, 127.4, 129.0, 129.5, 130.3, 132.2, 133.5, 133.9, 135.8, 141.6, 148.2, 148.6, 165.6; ESI MS (M+1): 363, (M–1): 361; HRMS, exact mass calcd for  $C_{21}H_{16}ClN_3O$ : 361.0982. Found: 361.0974. Elemental analysis Calcd for  $C_{21}H_{16}ClN_3O$ : C, 69.71; H, 4.46; N, 11.61. Found: C, 69.52; H, 4.27; N, 11.44. **11**: 2-((5*H*-imidazo[4,5-*c*]pyridin-5-yl)methyl)-*N*-(4-chlorophenyl)benzamide; mp 181–183 °C,  $^1H$  NMR (400 MHz, DMSO-*d*<sub>6</sub>)  $\delta$ , ppm: 4.95 (s, 2H, CH<sub>2</sub>), 7.17 (d, *J* = 8.0 Hz, 1H), 7.21 (m, 1H), 7.26 (d, *J* = 8.4 Hz, 2H), 7.33 (d, *J* = 8.8 Hz, 1H), 7.40 (m, 1H), 7.55 (d, *J* = 8.4 Hz, 2H), 7.68 (s, 1H), 7.75 (d, *J* = 8.4 Hz, 1H), 8.39 (s, 1H), 8.55 (d, *J* = 8.8 Hz, 1H), 13.30 (br s, exch. D<sub>2</sub>O, 1H, NH);  $^{13}C$  NMR (100 MHz, DMSO-*d*<sub>6</sub>)  $\delta$ , ppm: 49.9, 112.6, 122.8, 126.1, 127.0, 128.5, 129.4, 130.3, 131.6, 133.4, 133.9, 135.7, 135.9, 139.8, 146.5, 147.1, 150.6, 165.2; ESI MS (M + 1): 364, (M – 1): 362; HRMS, exact mass calcd for  $C_{20}H_{15}ClN_4O$ : 362.0934. Found: 362.0924. Elemental analysis Calcd for  $C_{20}H_{15}ClN_4O$ : C, 66.21; H, 4.17; N, 15.44. Found: C, 65.96; H, 4.03; N, 15.22.5.

8. VEGFR tyrosine kinase inhibition was determined by measuring the phosphorylation level of poly-Glu-Ala-Tyr-biotin (pGAT-biotin) peptide in a homogeneous time-resolved fluorescence (HTRF) assay. Into a black 96-well Costar plate was added 2  $\mu$ l/well of 25 $\times$  compound in 100% DMSO (final concentration in the 50  $\mu$ l kinase reaction was typically 1 nM to 10  $\mu$ M). Next, 38  $\mu$ l of reaction buffer (25 mM HEPES, pH 7.5, 5 mM MgCl<sub>2</sub>, 5 mM MnCl<sub>2</sub>, 2 mM DTT, and 1 mg/ml BSA) containing 0.5 mmol pGAT-biotin and 3–4 ng KDR enzyme was added to each well. After 5–10 min preincubation, the kinase reaction was initiated by the addition of 10  $\mu$ l of 10  $\mu$ M ATP in reaction buffer, after which the plate was incubated at room temperature for 45 min. The reaction was stopped by addition of 50  $\mu$ l KF buffer (50 mM HEPES, pH 7.5, 0.5 M KF, and 1 mg/ml BSA) containing 100 mM EDTA and 0.36  $\mu$ g/ml PY20K (Eu-cryptate labeled anti-phosphotyrosine antibody, CIS Bio International) was added and after an additional 2 h incubation at room temperature, the plate was read in a RUBYstar TRF reader.
9. (a) McTigue, M. A.; Wickersham, J. A.; Pinko, C.; Showalter, R. E.; Parast, C. V.; Tempczyk-Russell, A.; Gehring, M. R.; Mroczkowski, B.; Kan, C. C.; Villafranca, J. E.; Appelt, K. *Structure* **1999**, *7*, 319; (b) Berman, H. M.; Westbrook, J.; Feng, Z.; Gilliland, G.; Bhat, T. N.; Weissig, H.; Shindyalov, I. N.; Bourne, P. E. *The Protein Data Bank, Nucleic Acids Res.* **2000**, *28*, 235–242.

10. In order to establish *N*-arylbenzamide pharmacophores essential for VEGFR-2 activity, we have prepared seven analogues (**39–45**) of the potent inhibitors **10** and **14** (see below).



- Of these, only the benzimidazole **44** (rigid isostere of the secondary amide bond in **10**) displayed marginal activity against VEGFR-2 ( $IC_{50} = 2.66 \pm 0.40$   $\mu$ M). Compounds **39** and **40** were also hydrolytically unstable upon storage in DMSO and screening media (LC–MS analysis). Substitution at the central benzene ring (naphthalene **41**) was not tolerated. Tertiary amide (**42**), ester (**43**), and 5-aryl benzimidazole derivative (**45**) were inactive in the enzymatic assay (PI < 20% at 10  $\mu$ M). Based on these observations, we concluded that both secondary amide and flexible benzylic linker are required for the activity of the *N*-arylbenzamide derivatives. In addition, we found that *N*-(4-chlorophenyl)benzamides modified with 5-membered heterocycles (imidazole and tetrazole) were inactive against both VEGFR-2 and VEGFR-1. This was presumably due to lack of interaction of the respective 2-((1*H*-azol-1-yl)methyl) group with the Arg1032 moiety.
11. Competition assays were conducted with varying concentrations (0–500  $\mu$ M) of ATP. Specifically, five different concentrations of [<sup>32</sup>P]ATP were incubated with VEGFR-2 in the absence,  $IC_{50}$  or  $IC_{90}$  concentration of the inhibitors for 45 min at RT. A double reciprocal graph of the degree of phosphorylation (1/cpm) against ATP concentration (1/[ATP]) was plotted. The data were analyzed by a non-linear least-squares program to determine kinetic parameters using GraphPad software. Determined  $K_i$  values for the five selected compounds are listed in Table 2.
12. (a) Hanahan, D.; Folkman, J. *Cell* **1996**, *86*, 353; (b) Folkman, J.; Klagsburn, M. *Science* **1987**, *235*, 442; (c) Zachary, I. *Biochem. Soc. Trans.* **2003**, *31*, 1171; (d) Eskens, F. *Br. J. Cancer* **2004**, *90*, 1.